Journal of Biomechanics 87 (2019) 142–149

Contents lists available at ScienceDirect

Journal of Biomechanics

journal homepage: www.elsevier.com/locate/jbiomech
www.JBiomech.com

Computational modeling of neuromuscular response to swing-phase robotic knee extension assistance in cerebral palsy

Zachary F. Lerner [a,b,*], Diane L. Damiano [c], Thomas C. Bulea [c]

[a] Mechanical Engineering Department at Northern Arizona University, Flagstaff, AZ 86001, USA
[b] Department of Orthopedics, University of Arizona College of Medicine - Phoenix, Phoenix, AZ 85003, USA
[c] Rehabilitation Medicine Department, Clinical Center, National Institutes of Health, Bethesda, MD 20892, USA

ARTICLE INFO

Article history:
Accepted 27 February 2019

Keywords:
Cerebral palsy
Knee exoskeleton
Crouch gait
Musculoskeletal modeling
Rehabilitation robotics
Spasticity

ABSTRACT

Predicting subject-specific responses to exoskeleton assistance may aid in maximizing functional gait outcomes, such as achieving full knee-extension at foot contact in individuals with crouch gait from cerebral palsy (CP). The purpose of this study was to investigate the role of volitional and non-volitional muscle activity in subject-specific responses to knee extension assistance during walking with an exoskeleton. We developed a simulation framework to predict responses to exoskeleton torque by applying a stretch-reflex spasticity model with muscle excitations computed during unassisted walking. The framework was validated with data collected from six individuals with CP. Framework-predicted knee angle at terminal swing was within 4 ± 4° (mean ± sd) of the knee angle measured experimentally without the addition of spasticity. Kinematic responses in two-thirds of the participants could be accurately modeled using only underlying muscle activity and the applied exoskeleton torque; incorporating hamstring spasticity was necessary to recreate the measured kinematics to within 1 ± 1° in the remaining participants. We observed strong positive linear relationships between knee extension and exoskeleton assistance, and strong negative quadratic relationships between knee extension and spasticity. We utilized our framework to identify optimal torque profiles necessary to achieve full knee-extension at foot contact. An angular impulse of 0.061 ± 0.025 $Nm{\cdot}s{\cdot}kg^{-1}{\cdot}deg^{-1}$ with 0.013 ± 0.002 $Nm{\cdot}kg^{-1}{\cdot}deg^{-1}$ of peak torque and 4.1 ± 1.9 $W{\cdot}kg^{-1}{\cdot}deg^{-1}$ peak mechanical power was required to achieve full knee extension (values normalized by knee excursion). This framework may aid the prescription of exoskeleton control strategies in pathologies with muscle spasticity. https://simtk.org/projects/knee-exo-pred/.

1. Introduction

Excessive knee flexion at foot contact is a hallmark characteristic of pathological gait patterns associated with Cerebral Palsy (CP), particularly crouch gait (Sutherland and Davids, 1993). Improving knee extension during the late-swing phase of walking remains an important clinical objective when treating individuals with crouch gait because a flexed knee at initial contact reduces step length and may contribute to sustained crouch throughout the remainder of the stance phase (Steele et al., 2010). Standard medical care, including surgery (Dreher et al., 2012), muscle injections (Corry et al., 1999), and physical therapy (Damiano et al., 2010), may improve walking ability in children with CP, but reduced knee extension during late-swing to early-stance often persists or recurs following treatment (Galey et al., 2017). Potential causes of reduced knee extension during late-swing include hamstring tightness or spasticity, altered contralateral stance-limb mechanics, and reduced ipsilateral push-off in terminal stance (Arnold et al., 2007; Bar-On et al., 2014; Gage, 1990).

The need for improved rehabilitation outcomes when treating neurologically-based gait disorders has led to the development of lower-extremity wearable exoskeletons (Dollar and Herr, 2008). Clinical device design and testing has primarily focused on addressing pathological gait patterns and improving walking economy (Awad et al., 2017; Bortole et al., 2015; Lerner et al., 2018). Despite these advances, significant challenges remain for application of robotic assistance to improve pathological gait, particularly in ambulatory populations, including: inertia and weight compensation due to weakness, accommodation of individual musculoskeletal deformities resulting in contractures or altered muscle lines of action, assuring that robotic assistance does not exacerbate instability, alignment challenges due to rotational deformities, and

* Corresponding author at: Mechanical Engineering Department, Northern Arizona University, Flagstaff, AZ 86001, USA.
E-mail address: Zachary.Lerner@nau.edu (Z.F. Lerner).

https://doi.org/10.1016/j.jbiomech.2019.02.025
0021-9290/

assuring safe application of assistive forces in the presence of spasticity.

Robotic knee extension assistance during late-swing may prove useful for treating crouch gait; with the lower-extremity more fully extended at initial foot contact, the knee extensor muscles may operate more effectively to maintain a more upright posture during the remainder of the stance phase (Steele et al., 2012b). Controlling robotic assistance for this goal is not trivial. An exoskeleton control strategy that imposes a strict kinematic trajectory for individuals with spasticity may be painful and risk injury to muscle tissue. Therefore, in a prior observational study (Lerner et al., 2017a), we sought to evaluate the potential for assistive perturbations provided from a knee exoskeleton to improve dynamic posture during the stance and swing phases of the gait cycle. While this approach was well tolerated and resulted in significant reductions in crouch measured during mid-stance, we observed minimal improvement in knee extension at initial contact as children with crouch gait walked with swing-phase only or combined stance and swing-phase knee extension assistance. The less-than expected improvement may have resulted from inadequate assistance, or either volitional or non-volitional resistance from the knee flexors. These observations motivate the need for an improved understanding of individualized responses to exoskeleton assistance during swing to guide gait training and prescription. If the observed responses were a result of volitional or non-volitional resistance to the exoskeleton, then swing-phase assistance may not be an effective treatment strategy for some patients or they may alternately require more assistance than initially anticipated. The ability to partition, in real-time, responses to assistance into volitional and non-volitional components may help determine whether increasing or decreasing assistance would maximize kinematic and neuromuscular outcomes.

The goals of this study were to develop and validate a modeling framework to investigate the role of volitional and non-volitional muscle activity in subject-specific neuromuscular responses to robotic knee extension assistance during swing, and determine optimal knee extension torque patterns needed to improve late swing-phase knee extension in children with crouch gait. Our primary hypothesis was that modeling velocity-dependent hamstring spasticity in conjunction with volitional muscle activity would improve predictions of the kinematic and neuromuscular responses to assistance during crouch gait. Establishing the relationships between knee exoskeleton assistance, hamstring spasticity, and resulting kinematic response may prove useful to tailor both robotic assistance and overall treatment strategies. For example, a model that segments responses to robotic assistance into volitional and non-volitional components can inform the design of individualized assistance profiles to minimize non-volitional response. The model may also provide insight enabling clinicians to focus rehabilitation on reducing volitional activity in response to the exoskeleton, thereby maximizing functional outcomes.

2. Methods

2.1. Participant and study information

Seven individuals with crouch gait from spastic diplegic CP completed a six-visit feasibility study at the National Institutes of Health (NIH) Clinical Center (Lerner et al., 2017a). We obtained informed assent for each participant and written consent from their parents. Inclusion criteria included a Gross Motor Function Classification System level of I or II and the absence of knee flexion or extension contracture limiting normal range of motion during walking. Exclusion criteria included any health condition, besides CP, that could impact safety. The NIH Institutional Review Board approved this study. Over the first several visits, participants practiced walking with powered knee extension assistance, for a total assisted walking time of 50–100 min, depending on ambulatory ability. Experimental data used in this study were collected on the sixth visit as participants walked in two conditions: (1) with exoskeleton knee extension assistance during late swing (assisted) and (2) while wearing the exoskeleton but without assistance (unassisted); walking duration prior to experimental collection is noted in Table 1. Baseline data (walking without the exoskeleton) are reported in (Lerner et al., 2017b); we observed no significant difference in knee angle at initial contact between unassisted and baseline walking. Condition order was randomized across participants. One participant did not complete an exoskeleton walking trial under the unassisted condition, a requirement for this study; therefore, six participants were analyzed (Table 1). Surgical histories are reported in Supplemental Table 1.

2.2. Knee exoskeleton

The exoskeleton was comprised of a motor assembly mounted to custom-molded orthotics; see (Lerner et al., 2017c) for full details. Foot sensors and knee angle encoders informed a state machine that distinguished the stance, early swing, and late swing phases of gait. Late swing assistance started when the knee angular velocity transitioned from positive (flexion) to negative (extension) and terminated at heel strike. Extension torque during late-swing was programmed as a simple square-wave and tuned for each subject to a level that was well-tolerated and within device capability (12 Nm). The exoskeleton operated under zero-torque control to compensate for device friction and inertia about the knee joint during stance and early swing for the assisted condition and at all times during the unassisted condition. The unassisted exoskeleton trials were used so that we could isolate the effects of external assistance independent of the effects of device mass.

2.3. Experimental data

We used an established marker-set (Kwon et al., 2012) and a 10-camera motion capture system (Vicon) to record kinematic data as participants walked on an instrumented treadmill (Bertec). A wireless electromyography system (Trigno, Delsys) recorded activity of the vastus lateralis and lateral hamstring. Muscles were selected on the basis of being a major contributor to knee flexion-extension and EMG electrodes were placed based on SENIAM guidelines. Semitendinosus was targeted for knee flexion but in some cases electrode placement was shifted slightly due to device interference and may have reflected semimembranosus or biceps femoris activity. All EMG signals were verified by manual muscle testing before data collection. Participants walked at their preferred treadmill speed for a minimum of 30 s under each condition before data were collected. Kinematic and kinetic data were low-pass filtered at 6 and 12 Hz, respectively. Electromyography data were band-pass filtered (15–380 Hz), full-wave rectified, and low-pass filtered (7 Hz) to create a linear envelope (Lerner et al., 2016).

2.4. Musculoskeletal model

We used a previously published musculoskeletal model (DeMers et al., 2014) developed for simulating human gait in OpenSim (Delp et al., 2007); see supplemental material for additional detail. Peak isometric muscle force was scaled by height-squared to account for the relationship between a muscle's physiological cross-sectional area and height-squared (Jaric, 2002; Parker et al., 1990), an approach used previously in this population (Steele et al., 2012b). The musculoskeletal model was scaled to the

Table 1
Participant Information.

Patient (ID)	Gender	Age (yrs)	Height (m)	Body Mass (kg)	GMFCS[a] Level	MAS[b] (Spasticity)	Treadmill speed ($m \cdot s^{-1}$)	Assisted walking duration (s)	Unassisted walking duration (s)
P1	F	19	1.48	65.1	II	1	0.45	42	40
P2	M	12	1.72	69.3	I	1	0.50	66	57
P3	F	11	1.56	40.8	II	1+	0.50	67	52
P4	M	5	1.15	19.1	II	1	0.40	68	60
P5	M	11	1.35	32.0	II	2	0.70	66	40
P6	F	10	1.48	42.5	II	1+	0.50	75	74

[a] GMFCS: Gross Motor Function Classification Scale.
[b] MAS: Modified Ashworth Scale (clinical measure of spasticity) for the knee flexor muscles. Walking durations report the length of each assisted and unassisted walking trial and represent the acute (within-visit) acclimation time.

anthropometrics of each participant. We incorporated the inertial properties of each exoskeleton (motor assembly and custom orthotics) into each scaled musculoskeletal model; the exoskeleton's center of mass, center of mass location, and mass moments of inertia, were established from subject-specific computer-aided-design models.

Based on research indicating that spasticity is due to increased gain of the stretch reflex (Lance, 1980), we incorporated a stretch-reflex muscle controller (DeMers et al., 2017) in our model to account for spasticity-related changes in hamstrings activity due to powered assistance. Instantaneous muscle excitation ($e_{m\ total}$) was predicted for each hamstring muscle (semitendinosus, semimembranosus, biceps femoris long-head, biceps femoris short-head) according to (1):

$$e_{m\ total}(t) = e_m(t) + k_v\left(\dot{l}_m(t)\right) \tag{1}$$

where e_m was each muscle's excitation from computed-muscle-control (CMC) from OpenSim during unassisted walking, k_v was the gain on the normalized muscle stretch velocity, $\dot{l}_m$, which was computed as the ratio of current muscle fiber lengthening velocity, to the maximum contractile velocity of the muscle. Only muscle lengthening was incorporated. For this swing-phase analysis, our model did not include muscle length feedback, as in (Jansen et al., 2014), nor a threshold velocity as in (Van Der Krogt et al., 2016). The advantage of our approach was that it minimized the number of unknown model parameters requiring subject-specific fitting while remaining suitable for investigating velocity-dependent neuromuscular responses to assistance.

2.5. Predicting responses to exoskeleton assistance via simulation

We developed a novel simulation framework to evaluate the role of spasticity and volitional muscle activity in the measured kinematic responses to walking with knee-extension assistance (Fig. 1a). First, we determined the joint angles during the late swing-phase of each experimental walking trial (both assisted and unassisted) using inverse kinematics. OpenSim's Residual Reduction Algorithm (RRA) was used to minimize the dynamic inconsistencies (residual forces and moments, and model adjustments are reported in Supplemental Material). Next, we computed the muscle excitations from OpenSim's CMC analysis to compute each participant's underlying muscle activity that replicated measured whole-body dynamics during unassisted exoskeleton walking; CMC was conducted without control constraints or spasticity model. These excitations represented the net muscle activity underlying unassisted walking and potentially included non-volitional contributions. Employing the approach from (Steele et al., 2012a) to assess model validity, we qualitatively compared the computed muscle activity from CMC to those measured from electromyography for the unassisted walking trials for each participant (Fig. 2). We found good agreement for all participants, providing confidence in the excitations used in the forward dynamic simulations. The swing phases across conditions with the most similar peak knee flexion value at the start of late-swing were identified and analyzed for each participant.

Next, we applied the experimental exoskeleton torque measured via embedded torque sensors during assisted walking trials to the knee joint of each participant's musculoskeletal model driven by the muscle excitations computed as in Eq. (1) (i.e. excitations from unassisted walking plus the velocity-induced stretch reflex control for the hamstrings, if necessary). Excitations from CMC were not post-processed. The framework used experimental ground reaction forces (applied to the stance limb) from the same trial as the unassisted kinematic and muscle activity data to accomplish our goal of predicting responses from unassisted walking. If predicted knee extension exceeded the measured knee angle by 1° at terminal swing, the stretch-reflex controller velocity gain (k_v) was tuned by an optimization scheme that minimized the squared error between predicted and experimental knee angle at terminal swing.

2.6. Predicting optimal exoskeleton torque profiles

We used our simulation framework to determine an optimal torque signal that would result in full knee-extension at terminal swing (Fig. 1b). The objective function of our optimization algorithm sought to minimize the difference between the predicted knee angle at terminal swing and the desired knee angle (i.e. the angle at full extension), as well as the torque magnitude, as in (2):

$$(\theta_{optimized} - \theta_{desired})^2 + \left(\frac{peak\ \ torque^2}{scale\ \ factor}\right) \tag{2}$$

where $\theta_{optimized}$ was the knee angle at terminal swing resulting from each iteration of the optimization and $\theta_{desired}$ was the desired knee angle (0°) at terminal swing. For participants exhibiting a spastic response, the optimized torque signal was computed with and without incorporating the validated stretch reflex gains in our simulation to account for the anticipated neuromuscular response to the assistance. We used the Nelder-Mead simplex algorithm to optimize the torque control signal, approximated as a 3rd order spline function, by modulating the peak torque magnitude and temporal location (Fig. 1b). The spline was fit to 3 points. The start (1st point) and end (3rd point) of the optimized torque signal was constrained to zero. The x and y values (timing and magnitude) of the 2nd point were the optimization parameters. For the initial torque profiles, we specified a nominal level of 0.3 Nm/kg peak assistance at the mid-point of late-swing as it was the largest value applied in the experimental protocol (Lerner et al., 2017a). The scale factor (500) was used to prioritize convergence of the objective function on the minimization of the knee angle error, the primary goal of the optimization.

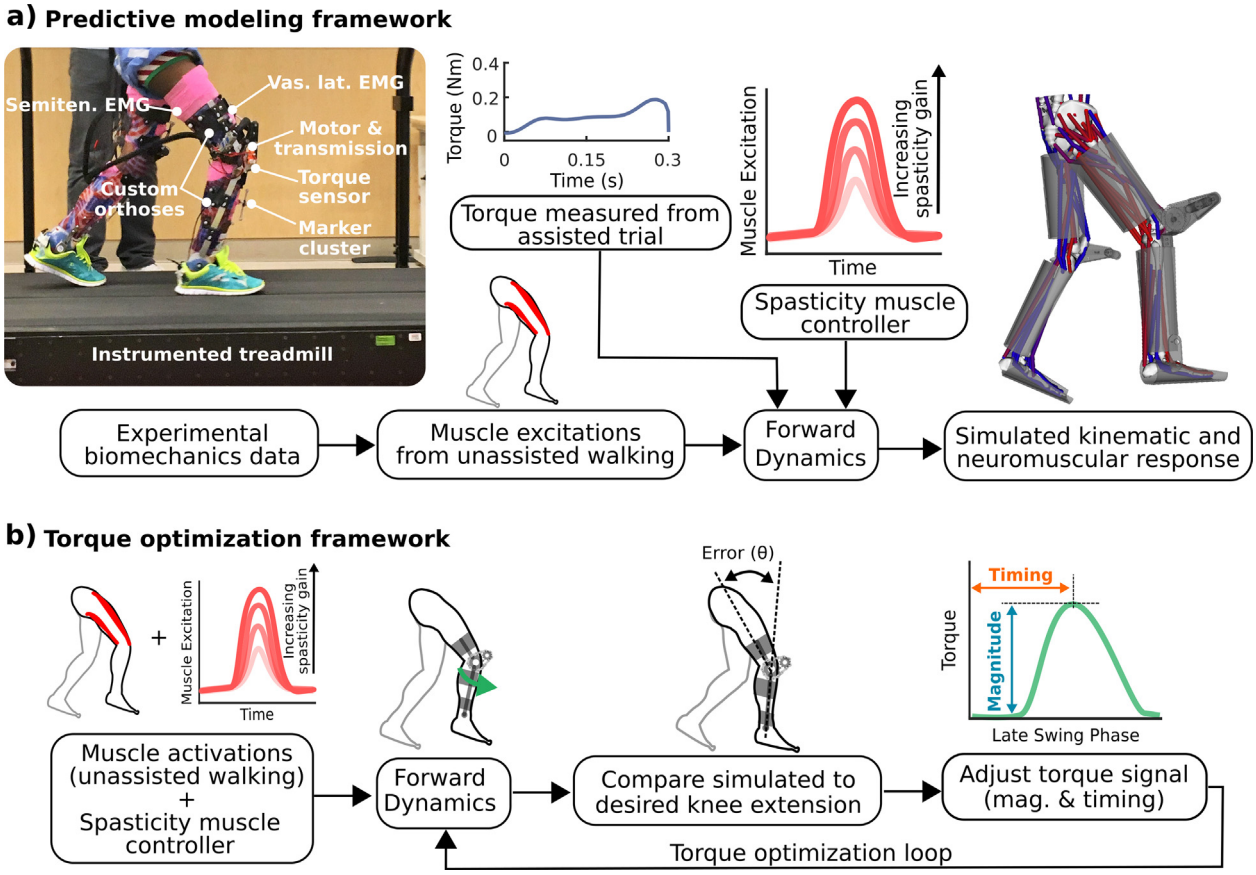

Fig. 1. Schematic depictions of the predictive modeling and torque optimization frameworks.

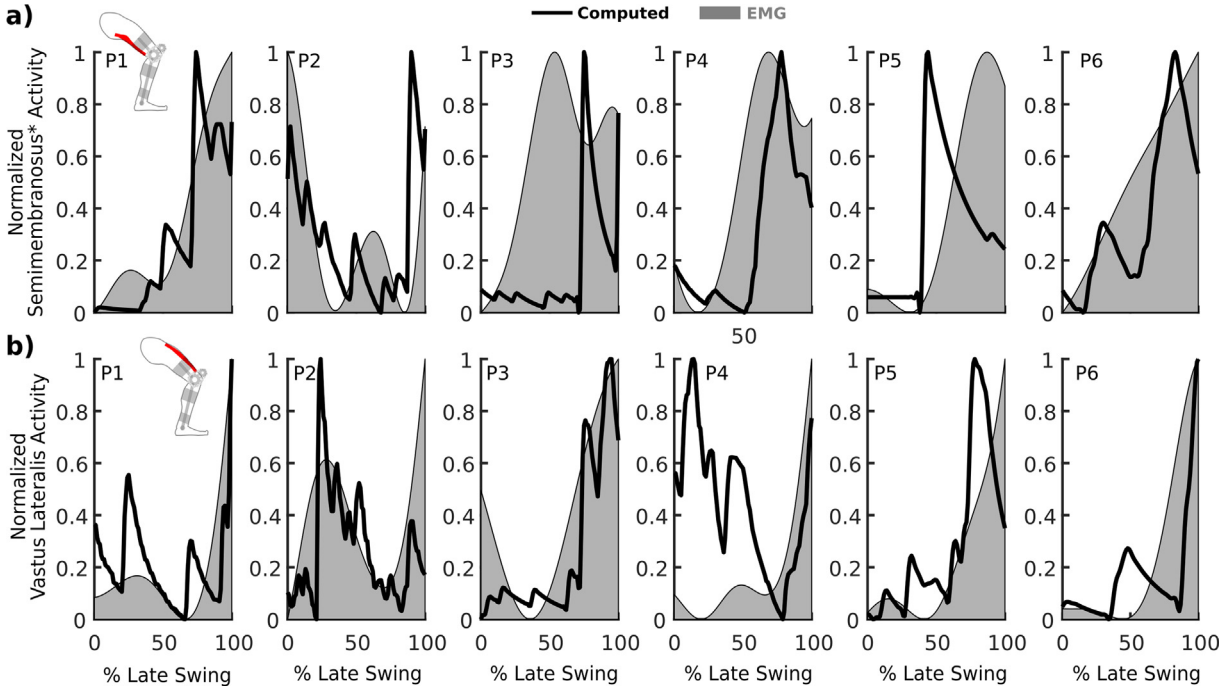

Fig. 2. Comparison of computed muscle activity (CMC, black lines) and measured muscle activity from EMG (gray shading) for the semimembranosus (a) and vastus lateralis (b) during the unassisted walking trials for each participant (P1-P6, columns 1–6). *Assessment revealed that the medial hamstrings EMG for participant P2 was located on the semitendinosus rather than the semimembranosus. Computed and measured muscle activity were scaled between zero and one based on the minimum and maximum value over the late swing phase. The observed discrepancies between EMG and computed activations (e.g. delayed onset of computed semimembranosus activity for P3 and early onset of computed vastus lateralis activity for P4) may be due to the fact that the optimization function used to determine individual muscle activations from CMC does not actively account for muscle co-contraction and may not account for differing neuromuscular characteristics of individuals with movement disorders.

2.7. Simulating the effect of spasticity on exoskeleton torque requirements

We performed regression analysis to quantify the relationships between simulated change in knee extension, applied torque (impulse), and hamstrings spasticity levels (stretch-reflex velocity gain). We generated simulations for all participants with the following combinations of assistance and spasticity gains: spasticity gains were varied between 0.0 and 1.0, at increments of 0.25, where the high end was slightly above the largest gain established experimentally; exoskeleton assistance was varied from 25% to 100% of the torque needed to fully extend the knee during swing, at 25% increments. Baseline muscle activity from the unassisted trials were included in all simulations.

2.8. Data processing and analysis

The time profile of kinematic, kinetic, and muscle activity data was normalized by percent late-swing phase. Measured electromyography and predicted muscle activity data were scaled to the maximum activity level from the investigated walking interval. We quantified framework accuracy as the absolute error between predicted and measured knee angle at terminal swing because of relevance to clinical decision making. We calculated the angular impulse (Nm·s) needed to fully extend the knee for each participant's optimized torque profile by normalizing by body mass and the amount of knee excursion ($Nm{\cdot}s{\cdot}kg^{-1}{\cdot}deg^{-1}$). Normalization by excursion was done because each participant's knee started at a unique position, and our goal was to determine the amount of angular impulse needed to extend the knee a set amount (e.g. one degree) for each person. We used regression analysis to determine the relationship between applied impulse and the induced change in knee extension across the range of hamstring muscles spasticity levels, where only significant terms ($p < 0.05$) were included in the model.

3. Results

The knee angle at terminal swing (i.e. foot contact) predicted from the modeling framework was $4 \pm 4°$ (mean ± std) without the addition of spasticity of the experimentally measured knee angle for the assisted walking trials across the six participants (Fig. 3). Spasticity was included in two of the six participants (P1 and P2) because the predicted knee angle exceeded 1° at foot contact. For participant P1, a stretch-reflex velocity gain of 0.87 increased kinematic accuracy by 11° at terminal swing and predicted a 102% increase in the average semimembranosus activity for the assisted walking trial over the unassisted trial, compared to a 79% average increase measured via electromyography (Fig. 4a). For participant P2, a stretch-reflex velocity gain of 0.38 increased kinematic accuracy by 6° and predicted a 15% increase in the average semitendinosus activity for the assisted walking trial over the unassisted trial, compared to a 25% average increase measured via electromyography (Fig. 4b). Semitendinosus and vastus lateralis profiles and coactivation data for all participants and conditions are included in Supplemental Material.

Utilizing our simulation framework to optimize an efficient torque signal necessary for each participant to achieve full knee-extension at foot contact (Fig. 5a), a mean angular impulse of

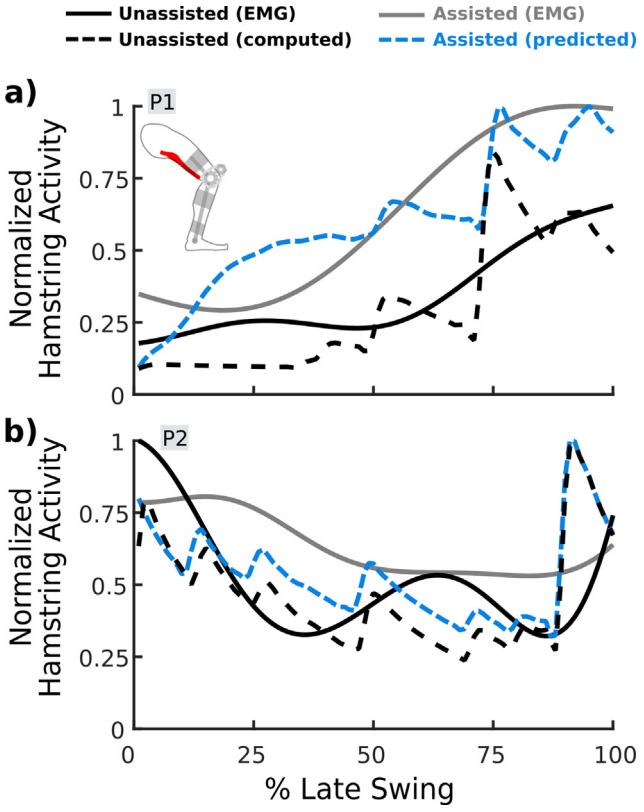

Fig. 4. Predicted increases in medial hamstring activity for P1 (a) and P2 (b) in response to exoskeleton assistance. The experimental torque profiles are presented in Fig. 5b row 2, columns 1 and 2.

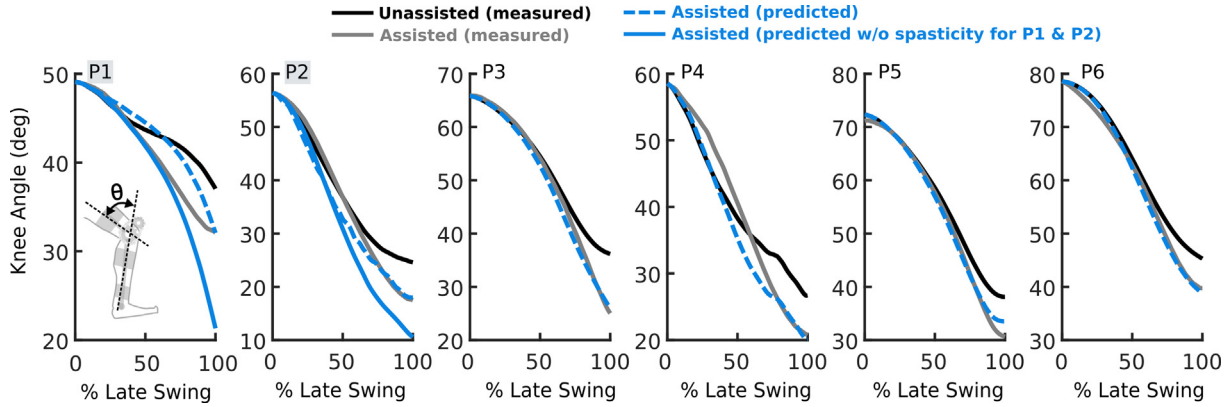

Fig. 3. Kinematic comparison of predicted and measured late swing-phase knee extension assistance for each participant (P1-P6, columns 1–6). Only the predictions for P1 and P2 were improved with non-zero spasticity terms; for reference, the kinematic predictions for these participants without spasticity (solid blue lines) are shown. (For interpretation of the references to colour in this figure legend, the reader is referred to the web version of this article.)

$0.061 \pm 0.025\ \mathrm{Nm{\cdot}s{\cdot}kg^{-1}{\cdot}deg^{-1}}$ with a mean peak torque of $0.013 \pm 0.002\ \mathrm{Nm{\cdot}kg^{-1}{\cdot}deg^{-1}}$ and mean peak power output of $4.1 \pm 1.9\ \mathrm{W{\cdot}kg^{-1}{\cdot}deg^{-1}}$ was required (Fig. 5b) across participants. Average hamstring muscle fiber lengthening velocity increased 113% from $0.13 \pm 0.04\ \mathrm{m{\cdot}s^{-1}}$ during unassisted walking to $0.27 \pm 0.1\ \mathrm{m{\cdot}s^{-1}}$ during the simulations resulting in full knee extension at foot-contact (Fig. 5c).

Regression analysis indicated strong relationships between simulated knee extension excursion, and angular impulse and spasticity, including an interaction between the angular impulse

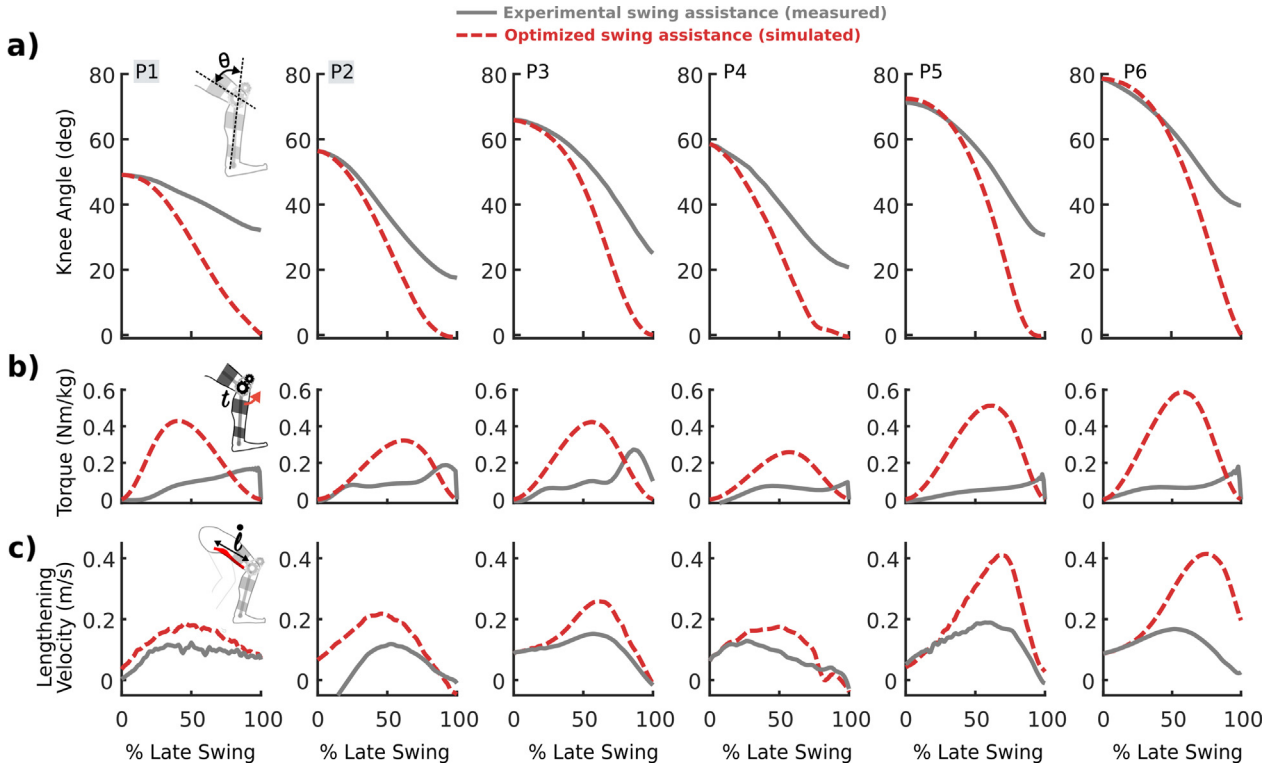

Fig. 5. Findings from the torque optimization scheme (red, dashed); comparison of late swing-phase knee kinematics (a), torque (b), and average hamstring muscle lengthening velocity (c) to those from the experimental study (gray, solid) for each participant (P1-P6, columns 1–6). The experimental knee angles and hamstrings lengthening velocity were determined from the inverse kinematics analysis of the experimental assisted walking trials. (For interpretation of the references to colour in this figure legend, the reader is referred to the web version of this article.)

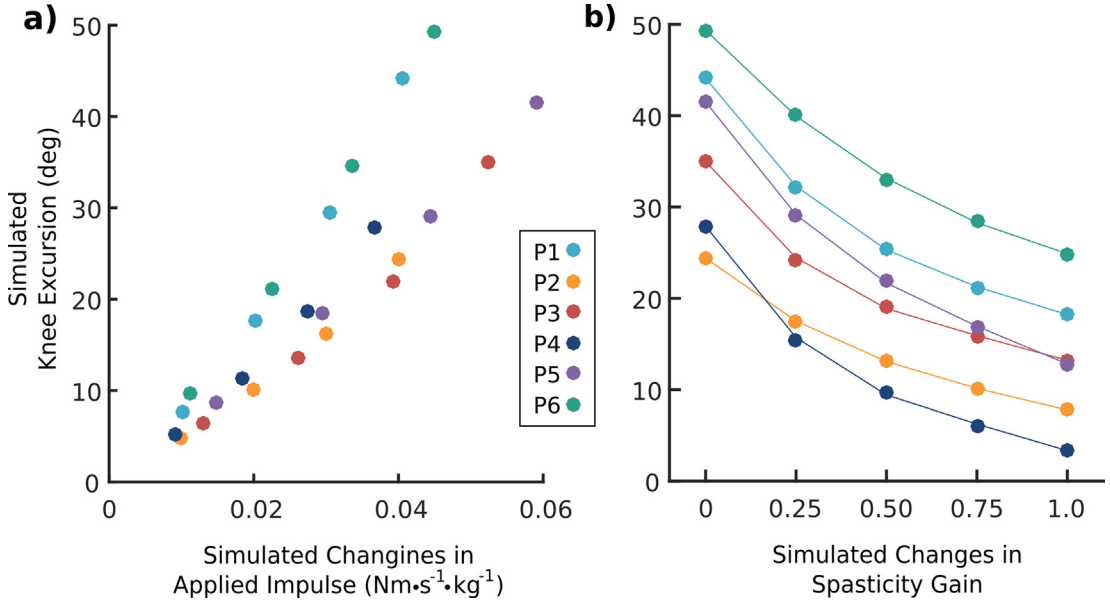

Fig. 6. (a) Simulated relationships between knee extension and amount of exoskeleton assistance when muscle spasticity was zero. Exoskeleton assistance was varied from 25% to 100% of the torque needed to fully extend the knee during swing, at 25% increments. (b) The isolated relationships between knee extension and velocity-induced hamstring spasticity when exoskeleton assistance was set at 100% of the torque needed to fully extend the knee across all participants.

and spasticity terms across all participants (Adjusted R^2: 0.78, RMSE: 5°). The regression equation estimated a change in knee extension (ΔKE), in degrees, as:

$$\Delta KE = -0.7 + 758.0I - 17.8k_v - 355.1(I \cdot k_v) + 12.1k_v^2 \quad (3)$$

where I represents the mass-normalized angular impulse ($Nm{\cdot}s{\cdot}kg^{-1}$) applied to the knee joint by the exoskeleton and k_v represents the stretch-reflex velocity gain (0–1). According to the model, knee extension increases linearly when spasticity is zero (e.g. 0.014 $Nm{\cdot}s{\cdot}kg^{-1}$ of applied angular impulse is required to extend the knee an additional 10° without spasticity, $k_v = 0$, Fig. 6a, R2: 0.77), while a quadratic relationship exists between spasticity gain and knee extension (i.e. low-level spasticity has a larger effect on change in knee extension compared to high-levels, Fig. 6b).

4. Discussion

We developed a predictive modeling framework to investigate subject-specific neuromuscular responses to knee extension assistance, and establish the relationships between powered assistance, velocity-induced hamstring spasticity, and late swing-phase knee extension. Our hypothesis that modeling velocity-dependent hamstring spasticity combined with volitional muscle activity would improve predictions of kinematic responses to knee extension assistance was only supported in a third of participants. Our simulations indicated that applied torque and underlying muscle activity was entirely responsible for the observed subject-specific kinematic for the remaining participants. Despite evidence that swing-phase assistive torque improved knee kinematics, we did not observe an improvement in underlying neuromuscular characteristics.

Modeling spasticity of the hamstring muscles improved kinematic predictions in one-third of the participants despite all participants having mild-to-moderate hamstring spasticity as assessed clinically by the Ashworth Scale. Since the Ashworth scale has shown good agreement with instrumented measures of the stretch response (Damiano et al., 2002), the amount of assistance provided during the experimental swing-assist trials was too low to trigger spasticity in some of the individuals that did not exhibit a spastic response. For this reason, we established the relationship between kinematic response, applied torque, and spasticity for all participants to account for the possibility that greater amounts of assistance would trigger a stretch-reflex in additional participants. These relationships may have practical implications for the clinical practice and experimental implementation of subject-specific assistance. For example, using an exoskeleton's torque and angle sensors, Eq. (3) can be used to solve for the stretch-reflex gain exhibited by the user during a trial with nominal assistance. This could inform whether a patient would be an appropriate candidate for additional training with swing-phase extension assistance, and if they are, determine the assistance needed to reach full extension in near real-time, from one gait cycle to the next. Future research is needed to investigate the potential existence of a threshold for spastic responses, and how that may be incorporated within the framework.

The hamstring muscle lengthening velocity required to reach full knee extension prior to initial contact (0.27 ± 0.1 $m{\cdot}s^{-1}$) for the participants in this study, including those exhibiting a spastic response, was found to be similar to the muscle lengthening velocity during normal walking in unimpaired individuals (0.3 $m{\cdot}s^{-1}$) (Agarwal-Harding et al., 2010). Our experimental and simulated findings demonstrate highly variable changes in coactivation as a result of assistance, with most, but not all, of the participants exhibiting an increase in the flexor contribution. These results reflect only a short duration of accommodation; improved responses (reduced coactivation) may occur with more practice. Still, it may be necessary to utilize strategies, such as muscle injections, and incentivized biofeedback (i.e. gamification techniques) to maximize volitional and non-volitional cooperation with powered assistance.

We found that the amount of knee extension assistance necessary to correct late swing-phase knee extension deficits in children with crouch gait was greater than anticipated. The torque and power requirements predicted from our analysis indicate that a larger, higher-power actuator, roughly three times heavier than those utilized in the present design, would be necessary for many participants to reach full knee extension. The framework can aid future designs and provide reasonable estimates of the best achievable posture given a motor's torque rating and an anticipated range of spasticity.

We estimated muscle excitations during unassisted walking trials using CMC, an approach that has been shown to produce realistic activations during walking in children with CP in this and other studies (Steele et al., 2013, 2010), yet may not reflect certain aspects of altered neuromuscular control. We assumed that participants did not actively fight exoskeleton assistance, as instructed. We ignored other factors beyond spasticity, such as altered passive muscle stiffness and contractures, that may affect the kinematic response to assistance. We modeled the interactions between the exoskeleton and body as rigid constraints, and the scaled models did not include subject-specific bony alignment. Because we focused our evaluation on a limited number of muscles, future modeling studies should more thoroughly investigate changes in activity across the lower-extremity and assess co-activation. Practical challenges associated with collecting EMG data from muscles located underneath exoskeleton attachment points is a reason why this modeling framework would benefit the field. Lastly, we assumed a linear relationship for velocity-dependent spasticity; future work should explore this assumption and additionally investigate non-linear relationships.

This study informs our understanding of exoskeleton requirements for improving swing-phase knee extension in individuals with CP, and helps establish the role of hamstring spasticity and volitional muscle activity in measured responses to powered knee extension assistance. We utilized our modeling framework to develop a predictive equation for determining subject-specific exoskeleton control parameters, which we anticipate will aid in the prescription of knee extension assistance and lead to improved functional outcomes.

Acknowledgment

This work was supported by Stanford University's National Center for Simulation in Rehabilitation Research (NCSRR) Pilot Project Program under NIH Grant R24HD065690, and by the Intramural Research Program of the NIH Clinical Center. We thank the OpenSim team, particularly Jennifer Hicks, PhD, Ajay Seth, PhD, Mathew DeMers, PhD, and Scott Delp, PhD, for assistance with this research and for making the utilized modeling tools publicly available.

Conflict of Interest

None declared for any authors on this manuscript.

Appendix A. Supplementary material

Supplementary data to this article can be found online at https://doi.org/10.1016/j.jbiomech.2019.02.025.

References

Agarwal-Harding, K.J., Schwartz, M.H., Delp, S.L., 2010. Variation of hamstrings lengths and velocities with walking speed. J. Biomech. 43, 1522–1526. https://doi.org/10.1016/j.jbiomech.2010.01.008.

Arnold, A.S., Thelen, D.G., Schwartz, M.H., Anderson, F.C., Delp, S.L., 2007. Muscular coordination of knee motion during the terminal-swing phase of normal gait. J. Biomech. 40, 3314–3324. https://doi.org/10.1016/j.jbiomech.2007.05.006.

Awad, L.N., Bae, J., O'Donnell, K., De Rossi, S.M.M., Hendron, K., Sloot, L.H., Kudzia, P., Allen, S., Holt, K.G., Ellis, T.D., Walsh, C.J., 2017. A soft robotic exosuit improves walking in patients after stroke. Sci. Transl. Med. 9. https://doi.org/10.1126/scitranslmed.aai9084.

Bar-On, L., Molenaers, G., Aertbelin, E., Monari, D., Feys, H., Desloovere, K., 2014. The relation between spasticity and muscle behavior during the swing phase of gait in children with cerebral palsy. Res. Dev. Disabil. 35, 3354–3364. https://doi.org/10.1016/j.ridd.2014.07.053.

Bortole, M., Venkatakrishnan, A., Zhu, F., Moreno, J.C., Francisco, G.E., Pons, J.L., Contreras-Vidal, J.L., 2015. The H2 robotic exoskeleton for gait rehabilitation after stroke: early findings from a clinical study. J. Neuroeng. Rehabil. 12, 54. https://doi.org/10.1186/s12984-015-0048-y.

Corry, I.S., Cosgrove, A.P., Duffy, C.M., Taylor, T.C., Graham, H.K., 1999. Botulinum toxin A in hamstring spasticity. Gait Posture 10, 206–210. https://doi.org/10.1016/S0966-6362(99)00037-5.

Damiano, D.L., Arnold, A.S., Steele, K.M., Delp, S.L., 2010. Can Strength training predictably improve gait kinematics? A pilot study on the effects of hip and knee extensor strengthening on lower-extremity alignment in cerebral palsy. Phys. Ther. 90, 269–279. https://doi.org/10.2522/ptj.20090062.

Damiano, D.L., Quinlivan, J.M., Owen, B.F., Payne, P., Nelson, K.C., Abel, M.F., 2002. What does the Ashworth scale really measure and are instrumented measures more valid and precise? Dev. Med. Child Neurol. 44, 112. https://doi.org/10.1017/S0012162201001761.

Delp, S.L., Anderson, F.C., Arnold, A.S., Loan, P., Habib, A., John, C.T., Guendelman, E., Thelen, D.G., 2007. OpenSim: Open-source software to create and analyze dynamic simulations of movement. IEEE Trans. Biomed. Eng. 54, 1940–1950. https://doi.org/10.1109/TBME.2007.901024.

DeMers, M.S., Hicks, J.L., Delp, S.L., 2017. Preparatory co-activation of the ankle muscles may prevent ankle inversion injuries. J. Biomech. 52, 17–23. https://doi.org/10.1016/j.jbiomech.2016.11.002.

DeMers, M.S., Pal, S., Delp, S.L., 2014. Changes in tibiofemoral forces due to variations in muscle activity during walking. J. Orthop. Res. 32, 769–776. https://doi.org/10.1002/jor.22601.

Dollar, A.M., Herr, H., 2008. Lower extremity exoskeletons and active orthoses: Challenges and state-of-the-art. IEEE Trans. Robot. https://doi.org/10.1109/TRO.2008.915453.

Dreher, T., Vegvari, D., Wolf, S.I., Geisbüsch, A., Gantz, S., Wenz, W., Braatz, F., 2012. Development of knee function after hamstring lengthening as a part of multilevel surgery in children with spastic diplegia: A long-term outcome study. J. Bone Jt. Surg. - Ser. A 94, 121–130. https://doi.org/10.2106/JBJS.J.00890.

Gage, J.R., 1990. Surgical treatment of knee dysfunction in cerebral palsy. Clin. Orthop. Relat. Res., 45–54

Galey, S.A., Lerner, Z.F., Bulea, T.C., Zimbler, S., Damiano, D.L., 2017. Effectiveness of surgical and non-surgical management of crouch gait in cerebral palsy: A systematic review. Gait Posture 54. https://doi.org/10.1016/j.gaitpost.2017.02.024.

Jansen, K., De Groote, F., Aerts, W., De Schutter, J., Duysens, J., Jonkers, I., 2014. Altering length and velocity feedback during a neuro-musculoskeletal simulation of normal gait contributes to hemiparetic gait characteristics. J. Neuroeng. Rehabil. https://doi.org/10.1186/1743-0003-11-78.

Jaric, S., 2002. Muscle strength testing: Use of normalisation for body size. Sport. Med. 32, 615–631. https://doi.org/10.2165/00007256-200232100-00002.

Kwon, S., Park, H.S., Stanley, C.J., Kim, J., Kim, J., Damiano, D.L., 2012. A practical strategy for sEMG-based knee joint moment estimation during gait and its validation in individuals with cerebral palsy. IEEE Trans. Biomed. Eng. 59, 1480–1487. https://doi.org/10.1109/TBME.2012.2187651.

Lance, J.W., 1980. Spasticity, disordered motor control. Chicago Year book Medical. https://doi.org/10.1136/jnnp.44.10.961.

Lerner, Z.F., Board, W.J., Browning, R.C., 2016. Pediatric obesity and walking duration increase medial tibiofemoral compartment contact forces. J. Orthop. Res. 34, 97–105. https://doi.org/10.1002/jor.23028.

Lerner, Z.F., Damiano, D., Bulea, T., 2017a. The effects of exoskeleton assisted knee extension on lower-extremity gait kinematics, kinetics, and muscle activity in children with cerebral palsy. Sci. Rep. 7. https://doi.org/10.1038/s41598-017-13554-2.

Lerner, Z.F., Damiano, D.L., Bulea, T.C., 2017b. A lower-extremity exoskeleton improves knee extension in children with crouch gait from cerebral palsy. Sci. Transl. Med. 9, 1–11. https://doi.org/10.1126/scitranslmed.aam9145.

Lerner, Z.F., Damiano, D.L., Park, H.S., Gravunder, A.J., Bulea, T.C., 2017c. A robotic exoskeleton for treatment of crouch gait in children with cerebral palsy: design and initial application. IEEE Trans. Neural Syst. Rehabil. Eng. 25, 650–659. https://doi.org/10.1109/TNSRE.2016.2595501.

Lerner, Z.F., Gasparri, G.M., Bair, M.O., Lawson, J.L., Luque, J., Harvey, T.A., Lerner, A. T., 2018. An untethered ankle exoskeleton improves walking economy in a pilot study of individuals with cerebral palsy. IEEE Trans. Neural Syst. Rehabil. Eng. https://doi.org/10.1109/TNSRE.2018.2870756.

Parker, D.F., Round, J.M., Sacco, P., Jones, D.A., 1990. A Cross-sectional survey of upper and lower limb strength in boys and girls during childhood and adolescence. Ann. Hum. Biol. 17, 199–211. https://doi.org/10.1080/03014469000000962.

Steele, K.M., DeMers, M.S., Schwartz, M.H., Delp, S.L., 2012a. Compressive tibiofemoral force during crouch gait. Gait Posture 35, 556–560. https://doi.org/10.1016/j.gaitpost.2011.11.023.

Steele, K.M., Seth, A., Hicks, J.L., Schwartz, M.H., Delp, S.L., 2013. Muscle contributions to vertical and fore-aft accelerations are altered in subjects with crouch gait. Gait Posture 38, 86–91. https://doi.org/10.1016/j.gaitpost.2012.10.019.

Steele, K.M., Seth, A., Hicks, J.L., Schwartz, M.S., Delp, S.L., 2010. Muscle contributions to support and progression during single-limb stance in crouch gait. J. Biomech. 43, 2099–2105. https://doi.org/10.1016/j.jbiomech.2010.04.003.

Steele, K.M., van der Krogt, M.M., Schwartz, M.H., Delp, S.L., 2012b. How much muscle strength is required to walk in a crouch gait? J. Biomech. 45, 2564–2569. https://doi.org/10.1016/j.jbiomech.2012.07.028.

Sutherland, D.H., Davids, J.R., 1993. Common gait abnormalities of the knee in cerebral palsy. Clin. Orthop. Relat. Res. 288, 139–147. https://doi.org/10.1097/00003086-199303000-00018.

Van Der Krogt, M.M., Bar-On, L., Kindt, T., Desloovere, K., Harlaar, J., 2016. Neuro-musculoskeletal simulation of instrumented contracture and spasticity assessment in children with cerebral palsy. J. Neuroeng. Rehabil. 13. https://doi.org/10.1186/s12984-016-0170-5.